Brain (1996), **119**, 701–708

Spinal cord atrophy and disability in multiple sclerosis

A new reproducible and sensitive MRI method with potential to monitor disease progression

N. A. Losseff, S. L. Webb, J. I. O'Riordan, R. Page, L. Wang, G. J. Barker, P. S. Tofts, W. I. McDonald, D. H. Miller and A. J. Thompson

NMR Research Unit, Institute of Neurology, London, UK

Correspondence to: Dr A. J. Thompson, NMR Research Unit, Institute of Neurology, Queen Square, London WC1N 3BG, UK

Summary

Recent MRI studies in multiple sclerosis have highlighted the potential importance of spinal cord atrophy (implicating axonal loss) in the development of disability. However, the techniques applied in these initial studies have poor reproducibility which limits their application in the serial monitoring of patients. The aim of this study was to develop a highly reproducible and accurate method for the quantification of atrophy. The technique we describe demonstrates an intra-observer coefficient of variation (scan–rescan) of only 0.8%. When applied to 60 patients with clinically definite multiple sclerosis there was a strong correlation between spinal cord area and disability measured by Kurtzke's Expanded Disability Status Scale (EDSS) ($r = -0.7$, $P < 0.001$). The correlation was graded providing evidence for a causal connection. At levels 3 and 8 of the EDSS we observed a reduction in average cord area of 12 and 35%, respectively. Given its reproducibility, the magnitude of the change detected and the strong correlation with disability, this new technique should prove to be a sensitive measure of progressive neurological deterioration and could be readily incorporated into imaging protocols aimed at monitoring therapy.

Keywords: multiple sclerosis; MRI; disability; spinal cord atrophy; clinical measurement

Abbreviations: EDSS = expanded disability status scale; SI = signal intensity; SRCC = Spearmann's rank correlation coefficient

Introduction

While conventional cranial MRI has been shown to be useful in predicting those with clinically isolated syndromes suggestive of multiple sclerosis who will go on to develop definite disease (Morrissey *et al.*, 1993; Filippi *et al.*, 1994), its relationship to the development of disability is more complex and at best limited (Thompson *et al.*, 1990; Kidd *et al.*, 1993; Filippi *et al.*, 1994, 1995*b*). This is likely to be due in part to the pathological heterogeneity of lesions which is not differentiated on conventional T_2-weighted MRI. More pathologically specific imaging techniques such as magnetization transfer imaging (Gass *et al.*, 1994) and spectroscopy (Arnold *et al.*, 1994; Davie *et al.*, 1996) have considerable potential, but it remains to be shown if they are sufficiently practical for inclusion in therapeutic trials as surrogate markers of neurological impairment.

Much of the disability that develops in multiple sclerosis is thought to be due to disease of the spinal cord, which is a common site of involvement (Oppenheimer, 1978). Using recent technical advances it has been possible to detect cord lesions readily on MRI (Kidd *et al.*, 1993). These studies have failed to show a cross-sectional or longitudinal relationship between disability and cord lesion load but have shown to varying degrees a relationship between spinal cord atrophy and disability (Kidd *et al.*, 1993; Filippi *et al.*, 1995*a*; Losseff *et al.*, 1995; Kidd *et al.*, 1996). In one study, patients with multiple sclerosis who had atrophy (defined as 2 SDs less than controls) at one or more of four spinal levels (C5, T2, T7 and T11), had significantly higher scores on the EDSS than those who did not have atrophy (Kidd *et al.*, 1993). Despite this relationship there was no significant difference

in cord area between less disabled subgroups of patients (relapsing–remitting and benign) and more disabled (primary and secondary progressive).

Another study concentrating on the C5 level has shown a significant difference in cord areas between patients with benign and secondary progressive multiple sclerosis (Filippi *et al.*, 1995*a*). A further longitudinal study of patients with primary and secondary progressive disease (Kidd *et al.*, 1996) showed a decrease in mean cord area over 1 year, but no definite correlation with disease progression. In addition, the changes seen in individual patients were within the 95% confidence limits for measurement variation.

The technique used in all these studies involved acquisition of axial sections of the spinal cord by a two-dimensional gradient echo sequence with manual outlining to calculate the cord area. This technique has poor scan–rescan reproducibility (coefficient of variation 6% in controls). Therefore, its suitability for the serial monitoring of progressive neurological impairment is very limited (Losseff *et al.*, 1995) as such poor reproducibility will obscure the detection of any change that may occur over a short period. We have analysed the reasons for this poor reproducibility and based on these have developed a new technique to measure atrophy of the spinal cord with anatomical, imaging and post-processing advantages.

Patients and methods

Sixty patients and thirty controls were recruited from the out-patient and in-patient departments and from staff members of the National Hospital for Neurology and Neurosurgery. All the patients studied had clinically definite multiple sclerosis according to recognized criteria (Poser *et al.*, 1983). All the controls were healthy volunteers. All subjects gave informed written consent to enter the study which had been approved by the ethical committee of the National Hospital for Neurology and Neurosurgery.

Of the 60 patients there were 15 in each of four clinical subgroups: relapsing–remitting, benign, primary and secondary progressive. These were defined as follows. (i) Relapsing–remitting: a history of relapses and remissions without gradual deterioration, but excluding benign cases. (ii) Benign: relapsing–remitting disease of at least 10 years duration and with disability on the EDSS of three or less. (iii) Primary progressive: progressive deterioration from the outset, without relapses or remissions for a period of at least 2 years. (iv) Secondary progressive: after an initial relapsing–remitting course, progressive deterioration for at least 6 months with, or without, superimposed relapses. All patients were randomly selected within the four subgroups and this is reflected in the distribution of EDSS scores. However, patients in a state of acute relapse were excluded from the study. Control subjects were selected to represent a wide range of age, height, weight and an equal sex distribution.

All patients were questioned and underwent a full neurological examination and evaluation of the Kurtzke EDSS score (Kurtzke, 1983) by one observer (N.A.L.). Following this, MRI of the spinal cord was performed. Control subjects answered a simple questionnaire regarding their general health and were excluded if any significant past or present illness was identified.

MRI protocol

All imaging was carried out on a Signa 1.5 T superconducting system (General Electric, Milwaukee, Wisc., USA) using phased array coils (Thorpe *et al.*, 1993). A volume acquired inversion prepared fast spoiled gradient echo acquisition was performed following an axial pilot at the level of the C7 vertebral body. Sixty-four partitions in the sagittal plane (x direction) of 1 mm thick equivalents were acquired in a three-dimensional volume centred on the cervical spine, with the following parameters: TI = 450 ms, TE = 4.2 ms, TR = 17.8 ms, flip angle = 20°, 256 phase encodings in the z direction, one average, field of view 25 cm, for both the z and y directions, matrix 256×256. The imaging time was 7 min.

Image post-processing

From the volume data set a series of five contiguous 3 mm pseudo axial slices were reformatted on the Signa using the centre of the C2/C3 intervertebral disc as a caudal landmark, with the slices perpendicular to the spinal cord.

Cross-sectional area measurement

The resulting images are illustrated in Fig. 1 showing two patients, one with benign and one with progressive multiple sclerosis. In view of the cord position and the strong signal intensity (SI) gradient between the cord (bright) and the surrounding CSF (dark) it was possible to apply a semi-automated measurement of the cord area as follows. The partial volume effect blurs the appearance of the boundary between the cord and CSF. If the cord and CSF were uniform in their composition then a contour drawn in the image at a SI halfway between the SIs of the cord and CSF would be at exactly the true position of the boundary. This is the basis of our method for locating the cord boundary, thus we must first determine the mean SI of the cord and CSF. Images were transferred to a Sun Workstation and uniformity corrected according to a previously described method (Tofts *et al.*, 1994). Following this, the images were blinded so the observer (N.A.L.) was unaware of their identity and then displayed, using the image display program Dispunc (D. L. Plummer, University College, London, UK). Windowing was standardized visually for all images against a single control image which was displayed at the same time. A region of interest was then drawn carefully around the

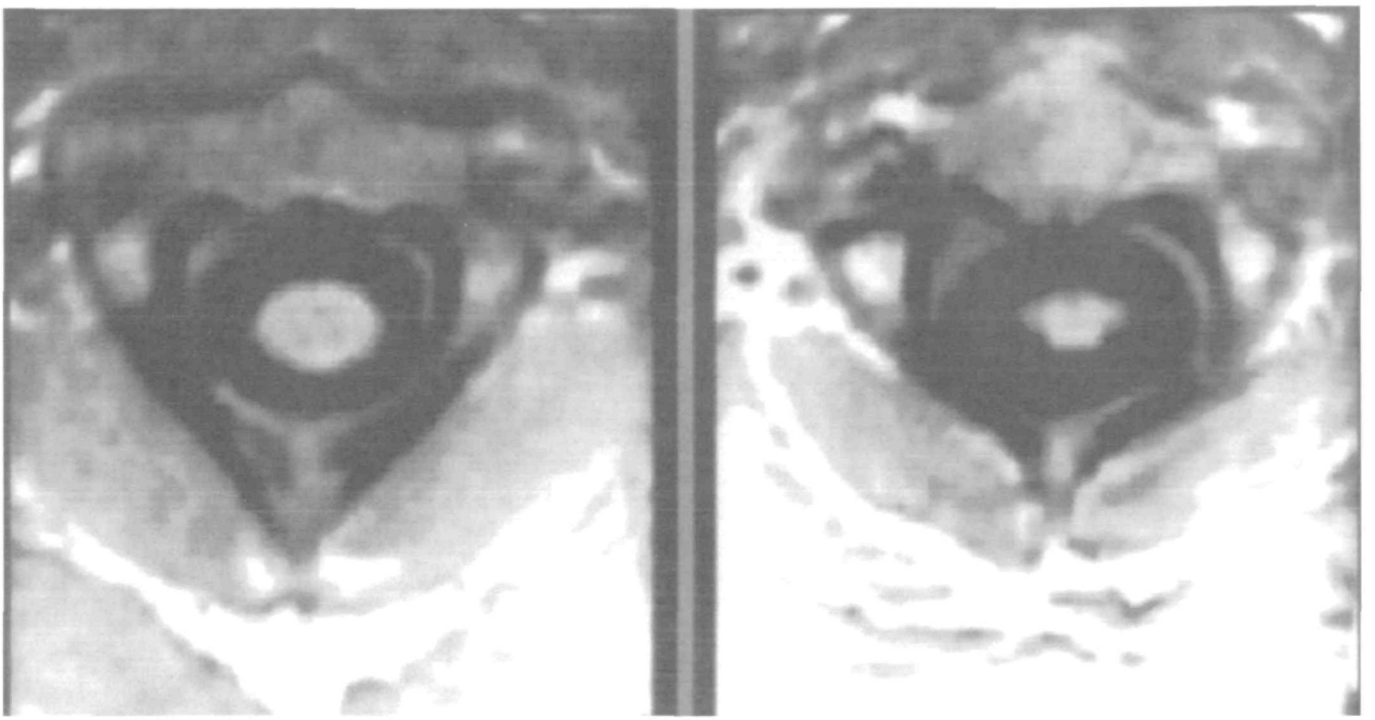

Fig. 1 Inversion prepared fast spoiled gradient echo acquisition at C2 in benign (*left*) and progressive (*right*) mutiple sclerosis. *Left*, female, age 46 years, disease duration 15 years, EDSS = 3, cord area = 85 mm^2. Right, female, age 31 years, disease duration 10 years, EDSS = 8, cord area = 55 mm^2. Patients are height- and weight-matched.

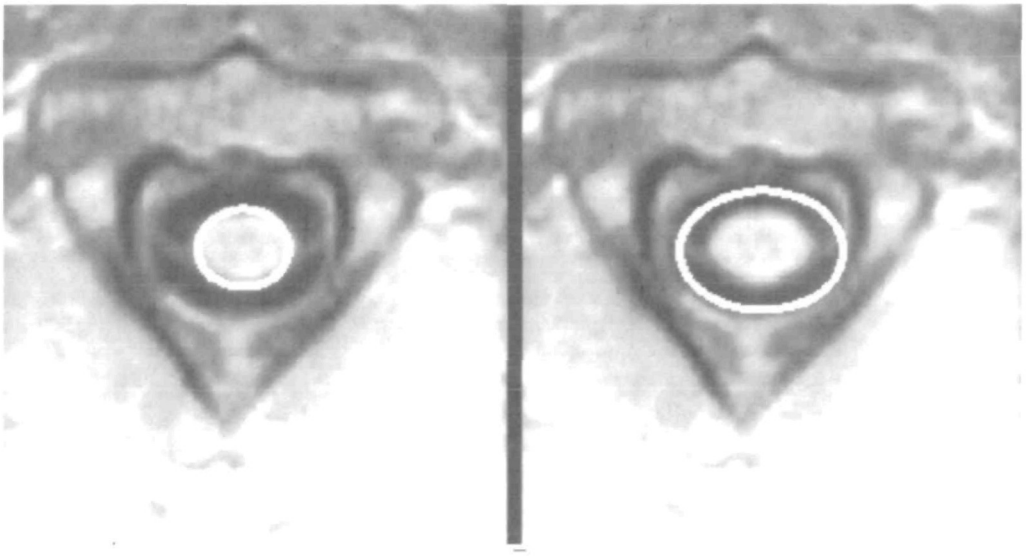

Fig. 2 *Left*, region of interest 'inner'. *Right*, region of interest 'outer'.

cord in the top slice (region of interest 'inner'), followed by a region of interest around the cord and CSF space (region of interest 'outer', illustrated in Fig. 2). From these two regions the mean CSF and cord intensities are calculated. The mean cord SI is the direct value from the first region of interest. The mean CSF SI is calculated by knowing the areas of the two regions of interest and their mean SIs. This is derived from the formula:

$$\text{mean CSF intensity} = \frac{(\text{mean SI outer} \times \text{area outer}) - (\text{mean SI inner} \times \text{area inner})}{(\text{area outer}) - (\text{area inner})}$$

The boundary SI is the mean of the cord and CSF SIs. The top slice is chosen to calculate the boundary SI, as this, in most cases, has the largest CSF space. This helps to minimize

inaccuracies that are inevitably present due to placement of the cord outline, which will affect the values in both regions of interest. Following this a seed is placed manually anywhere near the cord/CSF boundary and the computer then constructs an automated border around the spinal cord at the boundary SI previously calculated or as close as possible to it. This is performed for each of the five axial slices whose areas are then averaged.

Reproducibility

Reproducibility was assessed for both the post-acquisition measurement technique (i.e. calculating the cord area twice on the same image) and for scan–rescan (i.e. imaging the subject twice and then calculating the cord area from separate acquisitions), which is the realistic situation of a serial study. A series of 15 subjects (patients and controls) were selected to represent a range of spinal cord size. Each subject was scanned, removed from the magnet, repositioned and then rescanned. The images were then post-processed. The boundary SI calculations and area measurements were then made by two investigators, one experienced with the technique (having used it regularly and processed data from all the patients) and one not (no previous experience of the technique but a brief instruction on five different data sets beforehand).

Accuracy

Three cylindrical acrylic resin plastic rods of known dimensions were fixed in a water bath kept at room temperature. The rods were of uniform diameter to which the investigator was blind. These were imaged as above and five contiguous 3 mm slices were reformatted from the centre of the phantom. Uniformity correction was applied and, following this, contrast manipulation was performed to make the rods and surrounding water look as much like CSF and cord as possible.

To achieve this, the SI of the two compartments (CSF and cord) of the control image (from which all windowing is adjusted) was measured and the two ends of the window (maximum and minimum) were noted. In arbitrary units, the mean cord intensity = 21, mean CSF = 3, minimum window = 0 and maximum window = 40. From these figures the relative and absolute brightness of the phantom can be adjusted to appear as identical to the control image as possible. This is achieved by inverting the signal intensities, shifting and scaling to give realistic values of CSF/cord contrast and then adding gaussian noise to give realistic signal to noise ratios. Following this, measurement is made as above.

Statistics

Correlations between cord area and the EDSS were calculated using Spearmann's Rank Correlation Coefficient (SRCC) and Student's *t* test was used to evaluate the difference in cord areas between subgroups. Reproducibility was expressed as both the standard deviation of measurement variation (British Standards Institution, 1979) and the coefficient of variation (Goodkin *et al.*, 1992).

Table 1 *Intra-observer reproducibility measures*

	Same image	Scan/ rescan
Experienced	SD = 0.58 (0–1.9) CV = 0.73% (0–2.4)	SD = 0.63 (0.14–1.9) CV = 0.79% (0.2–2.5)
Inexperienced	SD = 0.83 (0–2.7) CV = 1.03% (0–3.4)	SD = 1.29 (0.1–5.6) CV = 1.61% (0.2–7%)

SD = standard deviation of measurement variation (mm^2);
CV = coefficient of variation.

Table 2 *Characteristics of patients and controls*

	Controls	All patients
Numbers	30	60
Mean age (years)	38	41
Range (years)	26–57	21–63
Male:female ratio	15:15	26:34
Mean height (m)	1.7	1.68
Range	1.4–1.95	1.48–2.15
Mean weight (kg)	65.6	65.7
Range	46–86	44–97
Cord area (mm^2)	84.7	74.3
Range	67–101	40–91

$P < 0.001$ for the difference in cord area between controls and patients.

Results

Reproducibility

The mean cord area of the 15 subjects was 85 mm^2 with a range of 45–101mm^2. The intra-observer standard deviation of measurement variation and coefficients of variation for the same scan and scan–rescan analysis are presented in Table 1. With an experienced observer the coefficient of variation for scan–rescan was 0.79%, standard deviation of measurement variation = 0.63 mm^2. Hence changes as little as 1.2 mm^2 (1.96 SDs) in cord area would be beyond the 95% confidence limits for a change that may have occurred simply because of measurement variation. There was no significant correlation between cord size and the individual coefficients of variation. The inter-observer variability was also low with coefficients of variation for the same image and scan–rescan analysis of 0.83 and 1.7%, respectively.

Accuracy

The known cross-sectional areas of the three acrylic resin plastic rods were 131.7 mm^2, 77 mm^2 and 49.6 mm^2

Table 3 *Individual patient subgroups*

	Primary progressive	Secondary progressive	Relapsing–remitting	Benign
Number	15	15	15	15
Mean age (years)	48.8	43.7	31	42.7
Range (years)	38–63	31–57	21–50	30–58
Mean disease duration (years)	10.4	15.9	4.1	14
Range (years)	2.5–24	4–30	1–10	10–20
Median EDSS	4	7	2.5	2
Range	2–7.5	4.5–8.5	1–6	1–3
Mean cord area at C2 (mm^2)	73.1	61.2	85.6	78.2
Range (mm^2)	48.3–88.8	44.8–72.2	74.1–95	60.8–92.3
P = from controls	<0.05	<0.001	n.s.	<0.05

n.s. = not significant.

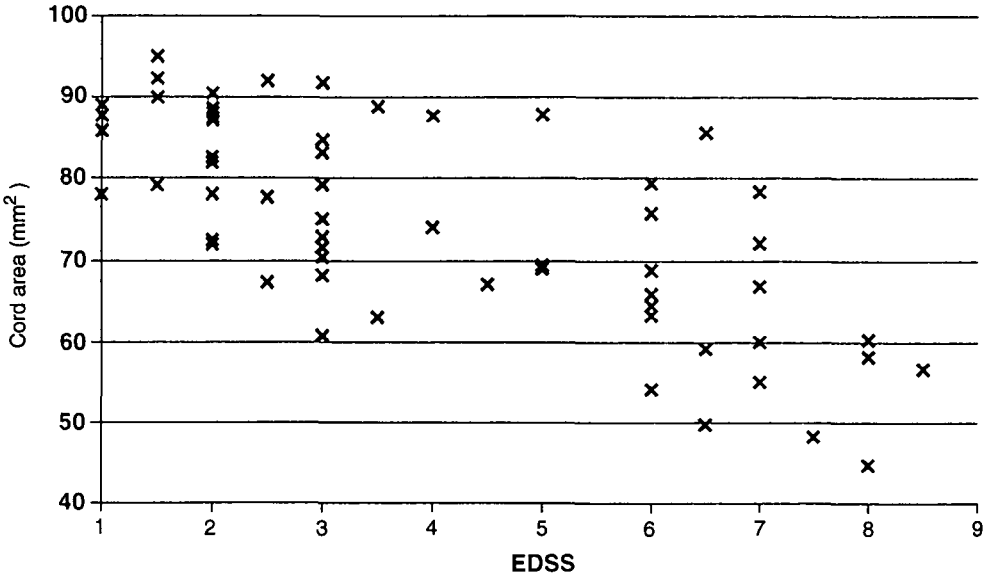

Fig. 3 Scatter chart of EDSS and C2 cord area in all patients (r = –0.7).

(mechanical measurement with a maximum uncertainty of 1%). Our imaging measurements were larger by 4.5%, 4.3% and 10.8%, respectively (measured values 137.7 mm^2, 80.4 mm^2 and 55 mm^2).

Controls

There were 30 controls whose characteristics are detailed in Table 2. There a was striking variation in cord size and no one factor was predictive. No significant correlation was seen between cord area and height, weight, body mass index or age. There were weak trends for increasing height and weight to correlate with increasing cord area [r = 0.36 and 0.28, respectively (SRCC)]. There was no relationship between age and cord area [r = –0.12 (SRCC)]. Female subjects had a smaller mean cord area than males (82.05 and 87.24 mm^2, respectively) but this difference was not significant (P = 0.11).

Patients

There were 60 patients whose characteristics are detailed in Tables 2 and 3. There was an extremely strong correlation between EDSS and cord area (*see* Fig. 3) [r = –0.7, $P < 0.001$ (SRCC)]. Significant correlations were also found when patients with high levels of disability were excluded [for the group EDSS 0–6, n = 40, r = –0.6, $P < 0.001$ (SRCC) and for the group EDSS 0–3, n = 33, r = –0.4, $P < 0.005$ (SRCC)]. At EDSS 3 the mean reduction in cord area compared with controls was 12% (n = 10), at EDSS 6 (n = 7) it was 21% and at EDSS 8 it was 35% (n = 3).

Significant correlation was also found between the functional system subscores of the EDSS, the EDSS itself and cord area, reflecting the tendency in most patients for subscores to increase as the disease progresses. The most significant correlations were between the functional system amidal and sphincter scores and cord area (r = –0.6 and

–0.66, respectively; $P < 0.001$, SRCC). Disease duration also correlated with cord area [$r = -0.52$, $P < 0.001$ (SRCC)].

There were significant differences in cord area between the whole patient group and controls ($P < 0.001$) and the individual subgroups of benign, primary progressive, secondary progressive when compared with controls ($P < 0.05$, < 0.05 and < 0.001, respectively).

There was no difference between controls and the early relapsing–remitting group most of whom had little disability. All patient groups were significantly different from each other ($P < 0.05$ to < 0.01) with the exception of benign versus primary progressive. Within the patient group the largest difference was seen between the early relapsing–remitting group and the secondary progressive group with mean cord areas of 85.63 mm^2 and 61.2 mm^2, respectively ($P < 0.01$).

Discussion

This study shows a strong graded correlation between a clinical measure of neurological impairment/disability (the EDSS) and spinal cord atrophy. This relationship is present across all levels of disability suggesting a causal relationship. More importantly the magnitude of change observed in the patients and the reproducibility of the measurement suggest that this technique (to measure spinal cord atrophy) may prove more sensitive in monitoring progressive neurological impairment/disability than other currently used imaging parameters. It may also provide a more sensitive index of meaningful change than the EDSS, especially in view of the poor test–retest reproducibility of this disability scale (Francis *et al.*, 1991). There are several reasons why this study has shown a stronger correlation with disability as measured by the EDSS than previous imaging studies. These reasons relate to the measurement technique, the specific area being measured and the nature of atrophy.

Technical factors

The high reproducibility of the newly developed technique relates to anatomical, imaging and measurement factors. A previous serial study (Losseff *et al.*, 1995) evaluating change in cord atrophy using a manual outlining technique following acquisition by two-dimensional proton density weighted gradient echo of single axial slices at four vertebral levels (C5, T2, T7 and T11) showed poor reproducibility. This poor reproducibility was not apparent from repeated measures on the same image (the coefficient of variation was 2%) but the magnitude of the problem became apparent once scan–rescan reproducibility was calculated (increasing the coefficient to 6%). This illustrates the considerable importance of assessing scan–rescan reproducibility for techniques that will be used to monitor change over time.

The poor reproducibility of the earlier method had several explanations. Imaging areas of the cord with marked local anatomical variability and therefore cross-sectional area measurement demands precise repositioning. This problem is most marked at the C5 level due to the cervical enlargement (Barson and Sands, 1977) and expansion of the cord associated with root outlets. At C5 in particular the CSF space is small leading to turbulent flow and CSF signal void. As in the thoracic region, the cord commonly abuts the bony canal and both these factors obscure the cord boundaries and lower the image contrast between the CSF and the spinal cord. Most images acquired at these levels by gradient echo could only be measured by a manual outlining technique and lack sufficient contrast for automated or threshold calculated contouring to work properly, which further decreases reproducibility. The C2 level offers several anatomical advantages. First the CSF space is wide and it is easy to position the patient (usually neck straight rather than in flexion or extension) so that the cord lies in the middle of the CSF pool. Thus cord/CSF contrast is maximized. Secondly, there is little variability in cross-sectional area of the cord over this segment. Hence slight repositioning errors have a minimal effect on scan–rescan reproducibility. Thirdly, unlike C5, it is an uncommon site for disc protrusion (Thorpe *et al.*, 1993).

Another important advantage of the new technique is the use of the volume acquired inversion prepared sequence. It achieves with the parameters described, excellent CSF suppression which enhances cord–CSF contrast and homogeneity of the cord and CSF compartments. It also allows post-acquisition reformatting of any slice prescription ensuring precise repositioning.

Finally we have used a semi-automated measurement technique to delineate the cord boundary which removes some of the imprecision that manual outlining and automated contouring have in delineating boundaries. In calculating the CSF image intensity by the method of one region (inner) within another (outer), errors of placement of the border that delineates the cord area and image intensity are counteracted: an overgenerous 'inner' cord boundary will lower the calculated cord SI but raise the calculated CSF SI and in contrast a small 'inner' cord boundary will increase the calculated cord SI and lower the calculated CSF SI. Thus, within a certain range, the technique produces a natural regression to the mean.

Our phantom experiments show that for normal size cords we probably overmeasure by ~4.5%. However the result from the smallest phantom shows overmeasurement by 10%. It is not surprising that overmeasurement increases as the structure gets smaller and this has been our visual impression of the *in vivo* situation. The greatest contribution to this inaccuracy is likely to be partial volume effects. As a structure gets smaller, the relative amount of partial volume that would be included in the first 'inner' region of interest increases, reducing the calculated mean SI of the cord and therefore lowering the calculated SI at which the border lies with consequent enlargement of the area. However, even with this bias, which works against the detection of smaller structures, we have shown a 35% reduction in the mean cord area of

patients with disability graded as EDSS 8 from controls. If this inaccuracy could be adjusted in some way (which should be possible with further phantom work) our measure of tissue destruction may become even more sensitive.

The spinal cord and disability

The EDSS is strongly weighted towards locomotion and hence more likely to correlate with destructive changes in the spinal cord than changes in the brain. The cervical cord is a common site for pathology in multiple sclerosis (Oppenheimer, 1978). However, previous studies of the cord in which the visible abnormality has been quantitated (areas of high signal on T_2-weighted scans) (Kidd *et al.*, 1993) have shown no relationship between these areas of high signal and clinical disability. This is likely to have been due to the non-specific nature of signal change detected by T_2-weighted conventional or fast spin echo and possibly failure to detect small lesions. The strong relationship between atrophy and disability (due to ataxia) has also been demonstrated in the cerebellum (Davie *et al.*, 1996).

What does atrophy signify?

The contribution of demyelination to atrophy is uncertain as reactive gliosis may, at least to some extent, fill the space previously occupied by myelin. However, Prineas (Prineas and Connell, 1978) has observed a reduction in axonal diameter associated with demyelination. Axonal loss is, of course, a potent cause of atrophy of the cord as studies of trauma show (Guttman, 1973). It is seen in many lesions in multiple sclerosis and may be extreme (Charcot, 1868; Bielschowsky, 1903; Dawson, 1916; Greenfield and King, 1936; Adams and Kubik, 1952; Ozawa *et al.*, 1994). Biopsies show it may occur acutely (Ozawa *et al.*, 1994) and it may be detected ophthalmoscopically as slits in the retinal nerve fibre layer early in the course of multiple sclerosis (Frisen and Hoyt, 1974) and even after a single episode of optic neuritis (W. I. McDonald, personal communication). There is indirect *in vivo* MRI evidence of axonal loss in chronic lesions derived from transverse magnetization decay curve analysis (Barnes *et al.*, 1991) and proton spectroscopy (Arnold *et al.*, 1992; Davie *et al.*, 1996). It is therefore likely that axonal loss makes a significant contribution to the atrophy we have observed, particularly when it is severe.

Two important issues remain to be addressed. One is the question of when detectable degrees of atrophy start to occur. In this study, we did not demonstrate a significant difference between the cohort of patients with early relapsing–remitting multiple sclerosis and controls. This cohort was characterized by a short disease duration (mean 4.2 years) and it is noteworthy that the benign group with a similar level of disability, but a much longer disease duration had a significant decrease in cord area. This suggests that atrophy may also be a feature of disease duration *per se*. To ascertain whether this measure will be of predictive value in early multiple sclerosis for future disability will require serial evaluation. Secondly, while there is a striking correlation between spinal cord atrophy and disability, we observed marked scatter at most levels of the EDSS. Whilst this may, in part, be due to natural biological variability, there remain some patients with marked disability (e.g. due to ataxia or involvement of the internal capsule) who do not have obvious spinal cord atrophy. It may be of considerable interest to study these patients with other regional area or volume measurements.

This results of this study demonstrate that spinal cord atrophy can now be measured with high serial reproducibility and that it is a clinically relevant entity. The consistent and marked changes in the spinal cord associated with disability underline the clinical relevance of measuring tissue destruction. This new technique could be easily incorporated into imaging protocols aimed at monitoring the effectiveness of putative therapies on pathological and clinical progression, not only in multiple sclerosis, but of other conditions characterized by progressive cord atrophy. A serial study is now needed to assess longitudinal change over time.

Acknowledgements

We wish to thank all those who volunteered for imaging and Mr D. MacManus, Miss H. Gallagher and Miss K. Birnie for carrying this out. The NMR Research Unit is funded by a generous grant from the Multiple Sclerosis Society of Great Britain and Northern Ireland. Dr Losseff is funded by a grant from the Brain Research Trust.

References

Adams RD, Kubik CS. The morbid anatomy of the demyelinative diseases. Am J Med 1952; 12: 510–46.

Arnold DL, Matthews PM, Francis GS, O'Connor J, Antel JP. Proton magnetic resonance spectroscopic imaging for metabolic characterization of demyelinating plaques. Ann Neurol 1992; 31: 235–41.

Arnold DL, Riess GT, Matthews PM, Francis GS, Collins DL, Wolfson C, et al. Use of proton magnetic resonance spectroscopy for monitoring disease progression in multiple sclerosis. Ann Neurol 1994; 36: 76–82.

Barnes D, Munro PM, Youl BD, Prineas JW, McDonald WI. The longstanding MS lesion. A quantitative MRI and electron microscopic study. Brain 1991; 114: 1271–80.

Barson AJ, Sands J. Regional and segmental characteristics of the human adult spinal cord. J Anat 1977; 123: 797–803.

Bielschowsky M. Zur histologie der multiplen sklerose. Neurol Zenbl 1903; 22: 770.

British Standards Institution. Precision of test methods I: guide for the determination and reproducibility for a standard test method (BS 5497, part 1). London: British Standards Institution, 1979.

Charcot JM. Histologie de le sclérose en plaques. Gaz Hop (Paris) 1868; 41: 554–5, 557–8, 566.

Davie CA, Barker GJ, Webb S, Tofts PS, Thompson AJ, Harding AE, et al. Persistant functional deficit in multiple sclerosis and autosomal dominant cerebellar ataxia is associated with axon loss. Brain 1996. In press.

Dawson JW. The histology of disseminated sclerosis. Trans R Soc Edin 1916; 50: 517–740.

Filippi M, Horsfield MA, Morrissey SP, MacManus DG, Rudge P, McDonald WI, et al. Quantitative brain MRI lesion load predicts the course of clinically isolated syndromes suggestive of multiple sclerosis. Neurology 1994; 44: 635–41.

Filippi M, Campi A, Colombo B, Martinelli V, Pereira C, Comi G. A spinal cord MRI study of benign and secondary progressive multiple sclerosis. In: Proceedings of The Society of Magnetic Resonance Third Scientific Meeting and Exhibition 1995a; 1: 277.

Filippi M, Paty DW, Kappos L, Barkhof F, Compston DA, Thompson AJ, et al. Correlations between changes in disability and T2-weighted brain MRI activity in multiple sclerosis: a follow-up study. Neurology 1995b; 45: 255–60.

Francis DA, Bain P, Swan AV, Hughes RAC. An assessment of disability rating scales used in multiple sclerosis. Arch Neurol 1991; 48: 299–301.

Frisen L, Hoyt WF. Insidious atrophy of retinal nerve fibers in multiple sclerosis. Funduscopic identification in patients with and without visual complaints. Arch Ophthalmol 1974; 92: 91–7.

Gass A, Barker GJ, Kidd D, Thorpe JW, MacManus D, Brennan A, et al. Correlation of magnetization transfer ratio with clinical disability in multiple sclerosis. Ann Neurol 1994; 36: 62–7.

Goodkin DE, Ross JS, Medendorp SV, Konecsni J, Rudick RA. Magnetic resonance imaging lesion enlargement in multiple sclerosis. Disease-related activity, chance occurrence, or measurement artifact? Arch Neurol 1992; 49: 261–3.

Greenfield JG, King LS. Observations on the histopathology of the cerebral lesions in disseminated sclerosis. Brain 1936; 59: 445–58.

Guttmann L. Spinal cord injuries: comprehensive management and research. Oxford: Blackwell Scientific, 1973: 78.

Kidd D, Thorpe JW, Thompson AJ, Kendall BE, Moseley IF, MacManus DG, et al. Spinal cord MRI using multi-array coils and fast spin echo. II. Findings in multiple sclerosis. Neurology 1993; 43: 2632–7.

Kidd D, Thorpe JW, Kendall BE, Barker GJ, Miller DH, McDonald WI, et al. MRI dynamics of brain and spinal cord in progressive multiple sclerosis. J Neurol Neurosurg Psychiatry 1996; 60: 15–19.

Kurtzke JF. Rating neurologic impairment in multiple sclerosis: an expanded disability status scale (EDSS). Neurology 1983; 33: 1444–52.

Losseff N, Lai M, Miller DH, McDonald WI, Thompson AJ. The prognostic value of serial axial cord area measurement by magnetic resonance imaging (MRI) in multiple sclerosis (MS) [abstract]. J Neurol 1995; 242 Suppl 2: S 110.

Morrissey SP, Miller DH, Kendall BE, Kingsley DP, Kelly MA, Francis DA, et al. The significance of brain magnetic resonance imaging abnormalities at presentation with clinically isolated syndromes suggestive of multiple sclerosis. A 5-year follow-up study. Brain 1993; 116: 135–46.

Oppenheimer DR. The cervical cord in multiple sclerosis. Neuropathol Appl Neurobiol 1978; 4: 151–62.

Ozawa K, Suchanek G, Breitschopf H, Bruck W, Budka H, Jellinger K, et al. Patterns of oligodendroglia pathology in multiple sclerosis. Brain 1994; 117: 1311–22.

Poser CM, Paty DW, Scheinberg L, McDonald WI, Davis FA, Ebers GC, et al. New diagnostic criteria for multiple sclerosis: guidelines for research protocols. Ann Neurol 1983; 13: 227–31.

Prineas JW, Connell F. The fine structure of chronically active multiple sclerosis plaques. Neurology 1978; 28: 68–75.

Thompson AJ, Kermode AG, MacManus DG, Kendall BE, Kingsley DPE, Moseley IF, et al. Patterns of disease activity in multiple sclerosis: clinical and magnetic resonance imaging study [see comments]. BMJ 1990; 300: 631–4. Comment in: BMJ 1990; 300: 1272.

Thorpe JW, Kidd D, Kendall BE, Tofts PS, Barker GJ, Thompson AJ, et al. Spinal cord MRI using multi-array coils and fast spin echo. I. Technical aspects and findings in healthy adults. Neurology 1993; 43: 2625–31.

Tofts PS, Barker GJ, Simmons A, MacManus DG, Thorpe J, Gass A, et al. Correction of nonuniformity in images of the spine and optic nerve from fixed receive-only surface coils at 1.5 T. J Comput Assist Tomogr 1994; 18: 997–1003.

Received December 12, 1995. Revised January 16, 1996.
Accepted February 16, 1996